A nonimmune function of T cells in promoting lung tumor progression

Jesse A. Green,[1,2,3]* Nicholas Arpaia,[1,2,3]* Michail Schizas,[1,2,3] Anton Dobrin,[1,2,3] and Alexander Y. Rudensky[1,2,3]

[1]Howard Hughes Medical Institute, [2]Immunology Program, and [3]Ludwig Center for Cancer Immunotherapy, Memorial Sloan Kettering Cancer Center, New York, NY

The involvement of effector T cells and regulatory T (T reg) cells in opposing and promoting solid organ carcinogenesis, respectively, is viewed as a shifting balance between a breach versus establishment of tolerance to tumor or self-antigens. We considered that tumor-associated T cells might promote malignancy via distinct mechanisms used by T cells in nonlymphoid organs to assist in their maintenance upon injury or stress. Recent studies suggest that T reg cells can participate in tissue repair in a manner separable from their immunosuppressive capacity. Using transplantable models of lung tumors in mice, we found that amphiregulin, a member of the epidermal growth factor family, was prominently up-regulated in intratumoral T reg cells. Furthermore, T cell–restricted amphiregulin deficiency resulted in markedly delayed lung tumor progression. This observed deterrence in tumor progression was not associated with detectable changes in T cell immune responsiveness or T reg and effector T cell numbers. These observations suggest a novel "nonimmune" modality for intratumoral T reg and effector T cells in promoting tumor growth through the production of factors normally involved in tissue repair and maintenance.

INTRODUCTION

The function of T cells within tumors has been a subject of intense research, in part because of the clinical success of blocking antibodies against inhibitory molecules on the surface of effector T cells. Furthermore, an increased presence of cytotoxic $CD8^+$ T cells and a high ratio of $CD8^+$ to Foxp3-expressing regulatory T (T reg) cells has been linked to improved clinical outcomes (Gooden et al., 2011; Fridman et al., 2012). Studies in this area centered primarily on the ability of αβT cells to respond to tumor antigens and mount an antitumor immune response resulting in tumor elimination. In analogy with infectious agents, tumors can escape T cell–mediated control through antigen down-regulation or mutation. In addition, the tumor microenvironment (TME) can limit antitumoral T cell responses in several ways, including impaired antigen presentation and immunomodulation. T reg cells suppress antitumoral T cell responses, and T reg cell depletion has been shown to restrain tumor growth in several cancer models in mice (Klages et al., 2010; Bos et al., 2013; Pastille et al., 2014).

Although much attention has been directed toward studying how conventional T cells respond to tumor antigens to limit tumor growth, and how restoring and boosting T cell responsiveness can result in effective cancer therapy, recent findings that T cells can also participate in tissue repair suggest that they may affect tumor growth in additional ways (Hofmann et al., 2012; Burzyn et al., 2013; Arpaia et al., 2015; Nosbaum et al., 2016; Sadtler et al., 2016). We hypothesized that $CD4^+$ T cells can support tumor growth through tissue repair–promoting activity in a manner that is independent of elaboration or suppression of antitumoral immune response. To test this hypothesis, we characterized the T cell populations within transplantable lung tumors in mice. We found that amphiregulin (Areg), an epidermal growth factor receptor (EGFR) ligand with important roles in organ development and tissue repair, was up-regulated in tumoral T cell populations. Using Lewis lung carcinoma (LLC) and EO771 breast carcinoma models, we found that T cell–derived Areg aided growth of developing tumors in the lungs, likely by acting on normal cells in the TME. The observed effect on tumor growth was not associated with changes in the number of intratumoral T cells or their ability to produce proinflammatory cytokines, suggesting that neither pan–T cell deficiency in Areg nor its selective loss in T reg cells had immunomodulatory effects on the TME. Our results suggest a novel "nonimmune" functional modality for intratumoral T cells in at least some forms of cancer—manifested by their ability to promote tumor growth through production of tissue repair and maintenance factors analogous to that of other tumor- and tissue-resident cells of hematopoietic and nonhematopoietic origin.

*J.A. Green and N. Arpaia contributed equally to this paper.

Correspondence to Alexander Y. Rudensky: rudenska@mskcc.org

N. Arpaia's present address is Dept. of Microbiology and Immunology, College of Physicians and Surgeons, Columbia University Medical Center, New York, NY.

Abbreviations used: Areg, amphiregulin; DT, diphtheria toxin; EGFR, epidermal growth factor receptor; LLC, Lewis lung carcinoma; rmAreg, recombinant mouse Areg; TME, tumor microenvironment.

The Rockefeller University Press
J. Exp. Med. 2017 Vol. 214 No. 12 3565–3575
https://doi.org/10.1084/jem.20170356

RESULTS AND DISCUSSION

Activated T reg cells accumulate within lung tumors and promote tumor growth

To explore potential effects of intratumoral T cell subsets in promoting the progression of tumors in nonlymphoid organs, we first compared the dynamics, phenotype, and function of T cell populations in lung tumors and normal tissue. Analysis of mice transplanted with syngeneic LLC and EO771 tumor cells, which grow aggressively in the lung to form macroscopic nodules at ∼14 d postinjection and typically lead to terminal disease by 28 d, showed increasing density of T reg cells and $CD4^+$ and $CD8^+$ effector cells in developing tumors (Fig. 1 A). Despite progressive decline in absolute T cell numbers likely caused by tumor necrosis, the percentage of intratumoral $Foxp3^+$ T reg cells among all $CD4^+$ T cells was increased relative to normal lung (Fig. 1 B). Consistently, T reg cells were highly proliferative, as determined by increased Ki-67 expression, and displayed an activated phenotype characterized by high levels of CTLA-4, PD-1, and GITR.

To assess a role of T reg cells in supporting LLC tumor growth, $Foxp3^{DTR}$ mice, in which T reg cells express the receptor for diphtheria toxin (DT) under the control of the endogenous *Foxp3* locus, were subjected to DT-mediated T reg cell ablation at days 11, 14, and 17 after tumor transplantation. T reg ablation resulted in a sizable reduction in tumor size at day 23–24 and a large influx of $CD4^+$ and $CD8^+$ T cells (Fig. 1, D and E), suggesting that T reg cells promote the growth of this poorly immunogenic lung carcinoma.

Areg production by lung tumor–resident T cells

We considered that in addition to limiting activation of T cells and innate immune cells, T reg cells may support tumor growth independently of immune modulation. Thus, we explored gene expression in intratumoral T reg and non–T reg cells using RNA sequencing (RNA-seq) to identify potential mediators of such an effect. Among genes up-regulated in T reg cells from tumors versus normal lung tissue, we identified several genes potentially involved in wound healing, including *Areg*, *Mmp12*, *Plau*, *Hpse*, and *Fn1*, and focused on *Areg* because of its known role in tissue repair (Berasain and Avila, 2014; Fig. 2 A).

Flow cytometric analysis performed directly after ex vivo T cell isolation showed that intratumoral T reg cells express increased levels of Areg relative to lung-resident T reg cells (Fig. 2 B). Furthermore, in vitro stimulation with PMA and ionomycin showed higher frequencies of Areg-producing T reg cells within the tumor compared with their counterparts in normal lung tissue (Fig. 2 C). In addition to T reg cells, after stimulation, intratumoral $CD4^+Foxp3^-$ effector T cells produced Areg at a noticeably higher frequency in comparison to those isolated from normal lung (Fig. 2 C).

Although the frequency of Areg production of T reg cells was much higher (Fig. 2 D), the numbers of Areg-producing T reg and effector $CD4^+$ T cells in the tumor were roughly equivalent (Fig. 2 E), whereas only few $CD8^+$ T cells were capable of Areg production in any setting tested. In addition to Areg-producing T cell subsets, several intratumoral myeloid cell subsets, including $Ly6C^+MHCII^-$ monocytes, $CD11b^+MHCII^+$ macrophages, and $CD11b^+Gr1^+$ neutrophils, were capable of Areg production. Although only a small percentage of cells within each myeloid cell subset produced Areg upon stimulation in vitro, the overall numbers of intratumoral myeloid cells capable of Areg production were roughly comparable to those of Areg-producing T cells (Fig. S1). Thus, several distinct populations of cells, including T reg and effector T cells, may contribute to the total level of Areg within tumors.

Areg produced by $CD4^+$ T cells contributes to lung tumor growth

Although seemingly dispensable under physiological conditions, Areg production by T reg cells has been demonstrated to play a role in tissue repair during viral lung infection without exerting a detectable effect on the immune response (Arpaia et al., 2015). To test whether T cell production of Areg affects lung tumor growth, we used $Areg^{FL/FL}$CD4-Cre and $Areg^{FL/FL}Foxp3^{YFP\text{-}cre}$ mice with a pan–T cell– or T reg–restricted Areg deficiency, respectively, transplanted with LLC and EO771. At days 21–24 after transplantation, LLC tumors in lungs of $Areg^{FL/FL}$ CD4-cre mice were significantly smaller than those in the lungs of littermate controls (Fig. 3 A). However, in $Areg^{FL/FL}Foxp3^{YFP\text{-}cre}$ mice, this reduction in tumor size was merely a non–statistically significant trend, suggesting that production of Areg by both T reg and non–T reg T cells may contribute to LLC growth in the lungs. EO771 tumors in the lungs of $Areg^{FL/FL}$CD4-cre mice were also smaller than in littermate controls (Fig. 3 B). In contrast to LLC, a significant, albeit lesser, reduction was observed in $Areg^{FL/FL}Foxp3^{YFP\text{-}cre}$ mice, suggesting that EO771 tumors have an increased sensitivity to Areg deficiency and that in this setting, production of Areg by T reg cells has a nonredundant role in tumor growth. Because several tumors are capable of Areg production, one possible explanation for the relative sensitivity of EO771, but not LLC, tumor progression to T reg cell–restricted Areg deficiency was a differing degree of Areg production by these cells. Indeed, we found that EO771 produced less Areg than LLC cells (Fig. S2 A). Upon transfer of LLC cells transduced with shRNA targeting Areg expression (Fig. S2 B) into $Areg^{FL/FL}Foxp3^{YFP\text{-}cre}$ mice and control littermates, overall tumor growth was unchanged relative to control shRNA-transduced LLC cells. Nevertheless, LLC cells expressing Areg shRNA showed a more pronounced trend toward reduced growth in $Areg^{FL/FL}Foxp3^{YFP\text{-}cre}$ mice that approached statistical significance, suggesting that Areg knockdown renders LLC cells somewhat more sensitive to the lack of T reg cell–produced Areg (Fig. S2 C). Thus, tumor cell–produced Areg may affect, if only very modestly, overall tumor growth or change the tumor cells' dependence on T reg cell–derived Areg for growth. To probe for a requirement for Areg production by T cells early during tumor develop-

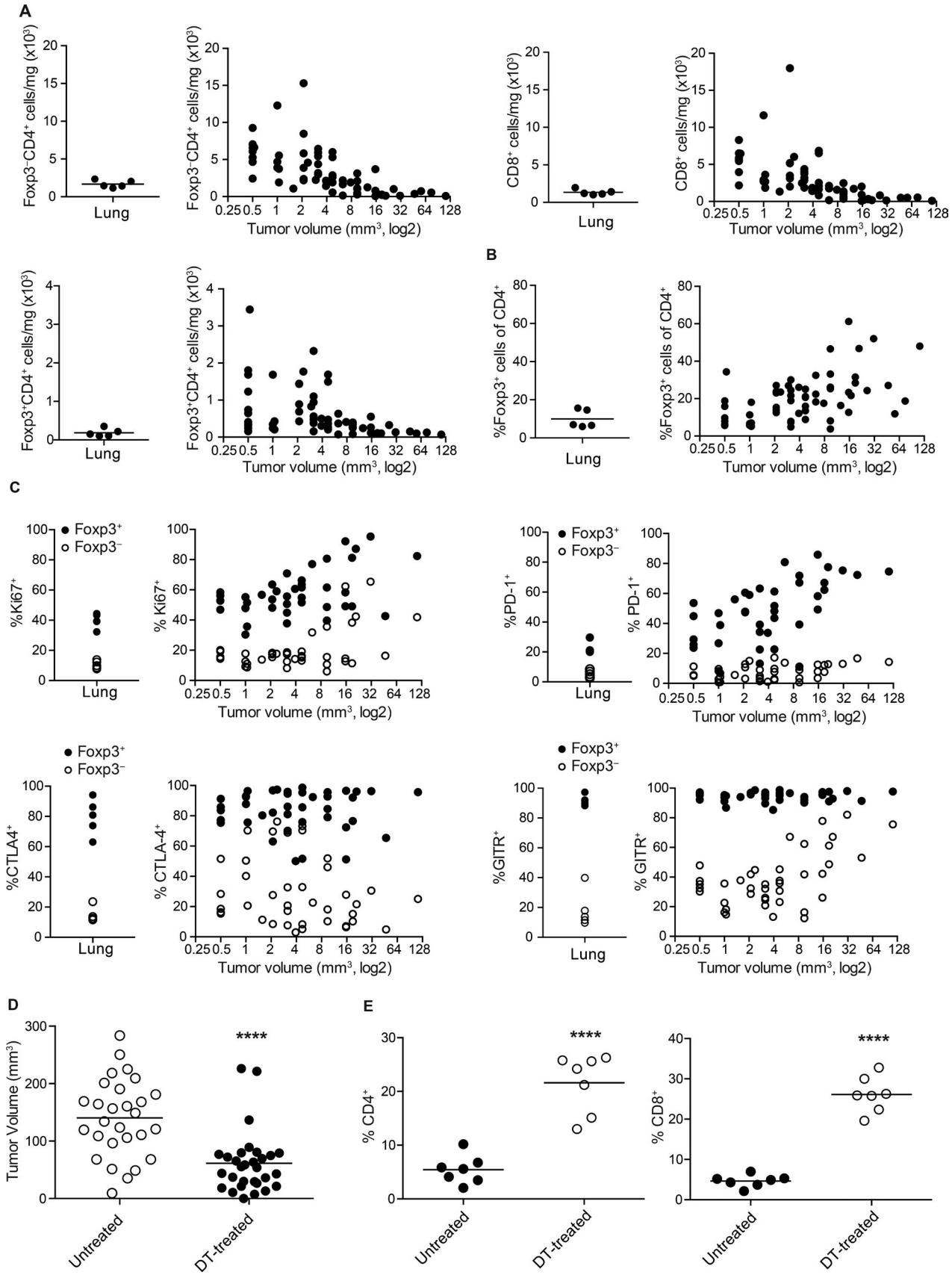

ment, we assessed the presence of GFP-tagged EO771 cells in the lung on day 5 after tumor transplantation, because EO771 tumors appeared most sensitive to Areg production. The comparable numbers of tumor cells observed in the lungs of *Areg*$^{FL/FL}$CD4-cre and littermate *Areg*$^{WT/WT}$CD4-cre or *Areg*$^{WT/FL}$CD4-cre controls (not depicted) suggested that T cell–derived Areg is dispensable for the very early steps in tumor colonization and niche formation in the lung, but rather is required at later stages of tumor development.

T cell–restricted Areg deficiency does not affect the tumor immune status

Because the ablation of T reg cells in *Foxp3*^{DTR} mice harboring LLC tumors caused a reduction in tumor size accompanied by a massive increase in activated CD4$^+$ and CD8$^+$ T cells within the tumor, we considered the possibility that T cell production of Areg may aid tumor growth by dampening the antitumor immune response. In fact, Areg has been suggested to act on EGFR expressed by Foxp3$^+$ T reg cells to increase their suppressive capacity (Zaiss et al., 2013). On the other hand, Areg-deficient Foxp3$^+$ T reg cells did not show a defect in their immunosuppressive capacity in vivo (Arpaia et al., 2015). To test whether Areg has an effect on the tumor immune status, we assessed the extent of T cell infiltration and cytokine production within LLC and EO771 tumors in the absence of T cell–derived Areg. Equivalent numbers of Foxp3$^+$ T reg cells, effector CD4$^+$ and CD8$^+$ T cells, and NK cells were present in LLC tumors from control and *Areg*$^{FL/FL}$ CD4-cre mice (Fig. 4 A and not depicted). In addition, T cell production of the proinflammatory cytokines IFNγ and TNFα was also unaffected in the Areg-deficient setting (Fig. 4 B). Because EGFR signaling in non–small cell lung cancer has been linked to increased PD-L1 expression (Zhang et al., 2016), which could negatively influence the antitumor T cell response, we assessed PD-L1 levels in LLC tumor cells in *Areg*$^{FL/FL}$CD4-cre mice and found them to be unchanged (not depicted). Likewise, T cell subset composition of EO771 tumors was unperturbed by the lack of Areg production by T cells, as reflected by both their numbers and the production of IFNγ and TNFα (Fig. 4, C and D). These results indicate that overall tumor immune status was not significantly changed in mice harboring Areg-deficient T cells and is unlikely to account for the decreased tumor growth observed.

Nevertheless, it remained possible that a small population of tumor-specific T cells could have mounted an increased antigen-specific response that inhibited tumor growth. To track antigen-specific responses, we took advantage of an engineered LLC cell line that expresses a transgene in which SIINFEKL peptide from the model tumor antigen ovalbumin (OVA) is coupled to H-2K^b and β2-microglobulin so that CD8$^+$ T cells can recognize this peptide (OVAp) presented by MHC class I (Hopewell et al., 2013). This tumor cell line enabled tracking of OVA-specific CD8$^+$ T cells within the tumor using OVAp-K^b tetramer staining as a way of measuring the tumor-specific T cell response. As with the parental LLC tumors, LLC-OVA tumor size was reduced in *Areg*$^{FL/FL}$ CD4-cre mice compared with littermate controls (Fig. 4 E). However, the numbers of OVA-specific CD8$^+$ T cells were unchanged (Fig. 4 F), and production of IFNγ and TNFα by effector CD4$^+$ and CD8$^+$ T cells was equivalent in tumors of *Areg*$^{FL/FL}$CD4-cre mice and littermate controls (Fig. 4 G).

T cell–derived Areg promotes tumor growth independently of signaling in tumor cells and alterations in vasculature

Diminished tumor growth accompanied by unperturbed proinflammatory cytokine production by intratumoral T cells and tumor-specific CD8 T cell responses in *Areg*$^{FL/FL}$ CD4-cre mice raised the question of whether T cell–derived Areg could be acting directly on the tumor cells. Both LLC and EO771 cells expressed EGFR and responded to recombinant mouse Areg (rmAreg) by increased phosphorylation of EGFR and Akt (Fig. S3 and Fig. 5 A). This observation was consistent with an idea that T cell–derived Areg could support tumor cell growth by signaling directly through EGFR on tumor cells. To directly test this possibility, we knocked down EGFR expression in EO771 cells upon infection with an EGFR shRNA–expressing retrovirus. As a control, cells were transduced with a retrovirus expressing Renilla luciferase shRNA. Phosphorylation of Akt upon stimulation with EGF or Areg was greatly reduced in EGFR shRNA–expressing cells (Fig. 5 A). However, EGFR-depleted and control EO771 cells formed similar size tumors in mice harboring Areg-sufficient T cells. Furthermore, EGFR-deficient and -sufficient EO771 cells yielded tumors comparably decreased in size in the absence of Areg produced by T cells in *Areg*$^{FL/FL}$CD4-cre mice (Fig. 5 B). In both EGFR and control shRNA–expressing tumors, the numbers of tumor-infiltrating CD4$^+$ and CD8$^+$ T cell populations and their production of effector cytokines were comparable (Fig. 5 C).

Figure 1. **Activated T reg cells accumulate within lung tumors and promote their growth.** (A–C) 150,000 LLC cells were injected i.v. into C57BL/6 mice, and tumors were analyzed from day 12 to 22. Individual tumor nodules as well as lungs from untreated mice were measured, weighed, and analyzed by flow cytometry. (A) T cell subsets in lungs and tumors of the indicated sizes. (B) Frequency of T reg cells among CD4$^+$ T cells. (C) Percentages of T reg cells and Foxp3$^-$CD4$^+$ T cells from lungs and tumors expressing indicated surface markers. In A–C, data represent individual tumors from 20 mice over three independent experiments. (D and E) 150,000 LLC cells were transplanted into *Foxp3*^{DTR} mice, which were treated with 0.5 µg DT or PBS (untreated) at day 11, 14, and 17. Tumors were analyzed at day 22–24. (D) Tumor sizes in PBS and DT-treated *Foxp3*^{DTR} mice; n = 25–30 mice per group pooled from four independent experiments; ****, P < 0.0001. (E) Percentages of tumoral CD4$^+$ and CD8$^+$ T cells among total cells. n = 7 mice per group; ****, P < 0.0001; representative of four independent experiments. In D and E, horizontal lines indicate the mean.

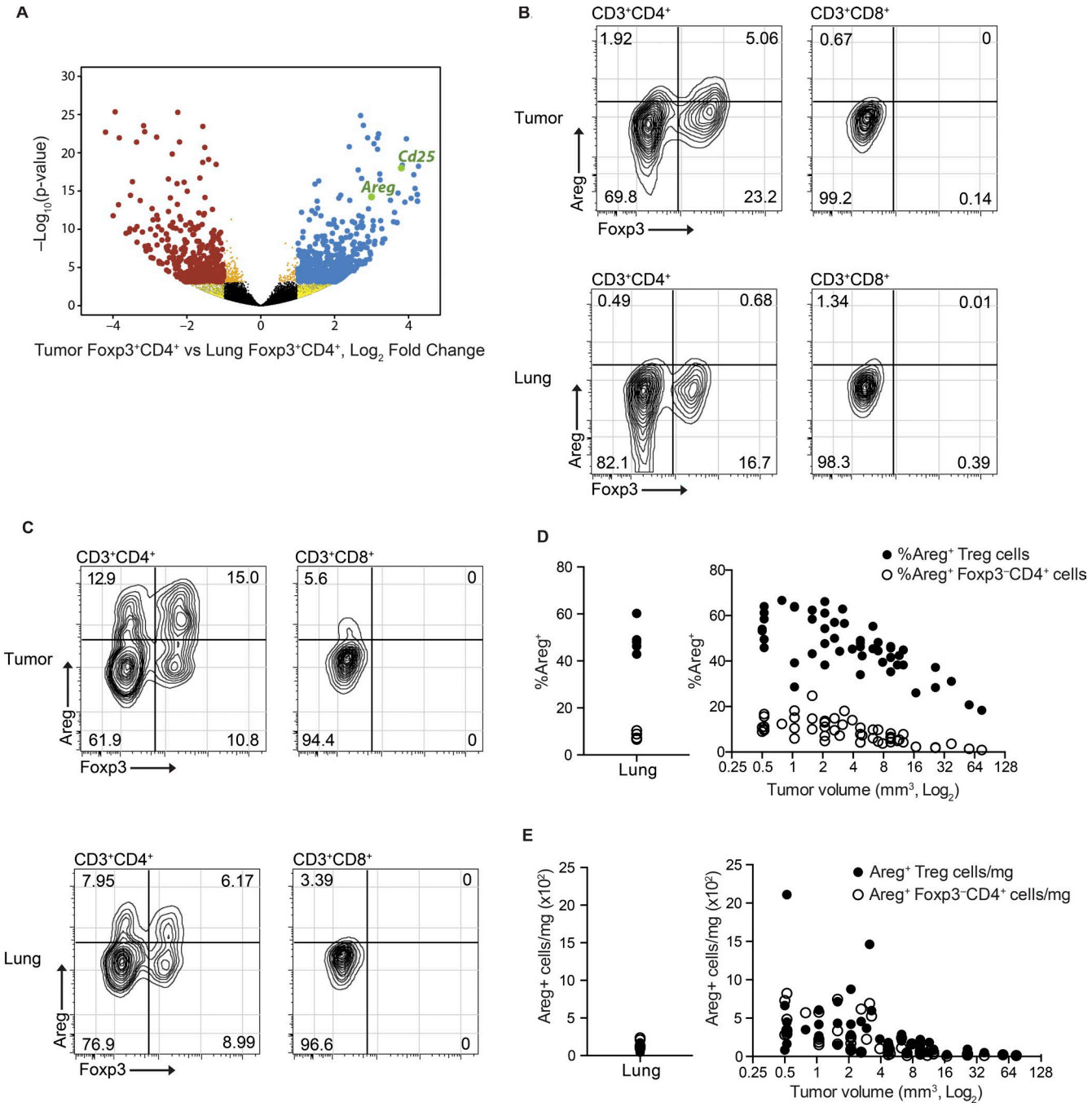

Figure 2. **Areg production by T reg and effector T cells in lung tumors.** (A) RNA-seq analysis of Foxp3$^+$CD4$^+$TCRβ$^+$ and Foxp3$^-$CD4$^+$TCRβ$^+$ T cells sorted from lungs and tumors of *Foxp3*^{GFP} mice on day 21 after i.v. injection of 150,000 LLC cells. Plot shows a comparison of genes expressed in Foxp3$^+$ T reg cells in tumors versus Foxp3$^+$ T reg cells in lungs. Genes significantly up-regulated (>2-fold) in tumor versus lung T reg cells are shown in blue; genes significantly down-regulated (>2-fold) are shown in black. A p-value of 0.01 was used for significance cutoff. Three biological replicates were analyzed. (B) Representative flow cytometry plots showing Areg expression in CD4$^+$ and CD8$^+$ T cells analyzed directly after isolation from LLC tumors or lungs of untreated mice. (C) Representative plots showing Areg expression in CD4$^+$ and CD8$^+$ T cells stimulated ex vivo with PMA and ionomycin for 3 h. (D) Percentages of Areg-expressing T reg and effector CD4$^+$ T cells stimulated ex vivo as in C. (E) Cell density of Areg-expressing T cell subsets from D.

Next, we sought to test whether growth of a tumor intrinsically incapable of responding to Areg might be sensitive to the lack of Areg production by T cells. B16-F10 melanoma cells, known to form tumor nodules in the lung when injected intravenously, did not express EGFR and failed to activate signaling pathways upon treatment with recombinant

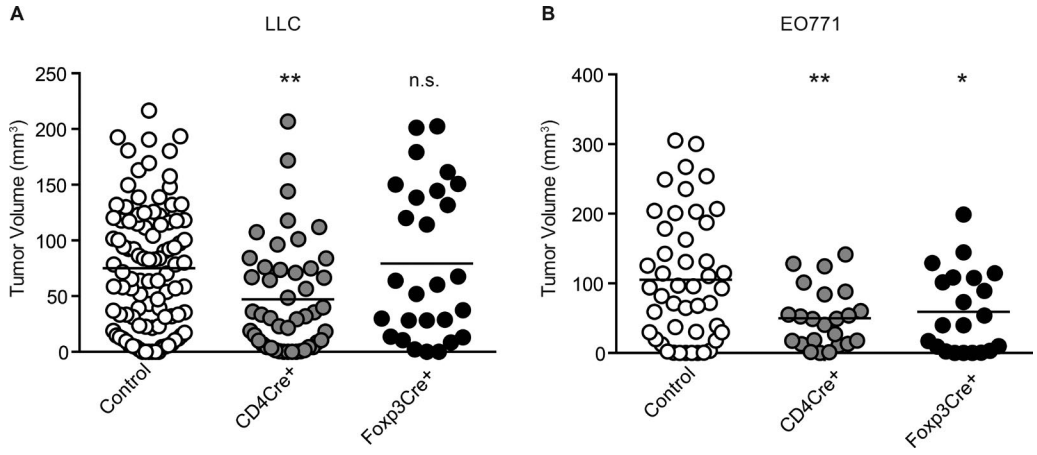

Figure 3. **T cell–derived Areg contributes to lung tumor growth.** (A) 150,000 LLC cells were injected i.v. into control (*Areg*$^{FL/FL}$ or *Areg*$^{FL/WT}$), *Areg*$^{FL/FL}$CD4-cre, and *Areg*$^{FL/FL}$*Foxp3*$^{YFP\text{-}cre}$ mice, and tumors were analyzed at day 22–24. Plot shows tumor volumes in mice of the indicated genotypes; $n > 25$ per group, pooled from five independent experiments; **, $P < 0.01$; n.s., not significant. (B) 150,000 EO771 cells were injected into mice as in A, and tumors were analyzed at day 22–26. Tumor size in mice of indicated genotypes is shown; $n > 14$ per group, pooled from at least three independent experiments; *, $P < 0.05$; **, $P < 0.01$.

mouse EGF or rmAreg in vitro (Fig. S3). Thus, we assessed the effects of T cell–restricted Areg deficiency on the growth of B16-F10 melanoma. Consistent with the results of our analysis of EGFR knockdown in EO771 breast carcinoma, B16-F10 melanoma cells also formed smaller-size tumors in *Areg*$^{FL/FL}$CD4-cre mice compared with littermate controls (Fig. 5 D). As with the other tumors tested, cytokine production by intratumoral B16-F10 T cells was unaffected by T cell–derived Areg deficiency (not depicted). These results suggest that direct signaling of Areg in tumor cells was unlikely to be responsible for the observed tumor-promoting effects of T cell–produced Areg and that T cell–derived Areg production likely supported tumor growth by affecting untransformed cells in the tumor-bearing lungs. We considered the possibility that T cell–produced Areg influenced the tumor environment by acting on stromal cells and potentially altering vascularization or extracellular matrix, thereby affecting the provision of nutrients or growth factors to the tumor. However, we found the overall amount of CD31$^+$ vascular endothelium and collagen IV distribution and the number of cleaved caspase-3–expressing apoptotic or Ki-67$^+$ dividing cells within the tumor to be largely unchanged in *Areg*$^{FL/FL}$ CD4-cre mice (not depicted). Thus, a yet-unidentified mechanism, which acts on nontransformed cells in the tumor microenvironment, leads to the observed attenuation of lung tumor growth resulting from Areg deficiency in T cells.

Studies of the role of T lymphocytes in cancer have mainly been framed by concepts of infectious immunity to infection and immunological tolerance (Chen and Mellman, 2013). Within the former framework, CD4$^+$ and CD8$^+$ T cells are poised to eliminate tumors by recognizing tumor neoantigens analogous to attack on pathogens, whereas tumors deploy a variety of immune evasion mechanisms ranging from a loss or down-modulation of T cell target antigens to a diverse means of immunomodulation.

Our studies indicate that through production of Areg, T reg and effector CD4$^+$ T cells can promote the growth of lung tumors. Although several studies have shown that an increased antitumor immune response after ablation of T reg cells or after treatment with checkpoint inhibitors that boost T cell activation can result in reduced tumor burden, we found that CD4$^+$ T cells can also promote tumor growth through the expression of a factor with an established role in tissue repair in a manner apparently independent of immune modulation. These findings are reminiscent of an earlier finding that effector CD4$^+$ T cells, likely specific for bacterial antigens, markedly enhanced neoplastic progression and tumor incidence in an HPV16 transgene–driven model of invasive squamous carcinoma in mice (Daniel et al., 2003). Likewise, T reg cells have been shown to provide RANK ligand to promote metastasis in an Erbb2-driven mammary carcinoma model (Tan et al., 2011).

There is growing evidence that T cells participate in tissue repair processes. In experimental models of muscle injury and myocardial infarction, CD4$^+$ T cells accumulate in the damaged tissue and contribute to regeneration (Hofmann et al., 2012; Sadtler et al., 2016). Ablation of T reg cells also inhibits the repair of damaged muscle tissue and healing after myocardial infarction (Burzyn et al., 2013; Weirather et al., 2014). Tissue repair and wound healing bear striking similarities to certain aspects of tumor growth, and it has long been speculated that tumors can exploit the wound healing response to gain a growth advantage (Schäfer and Werner, 2008).

By acting through EGFR, amphiregulin can promote tissue repair by stimulating fibrosis as well as the survival and proliferation of hepatocytes, intestinal epithelial cells, and

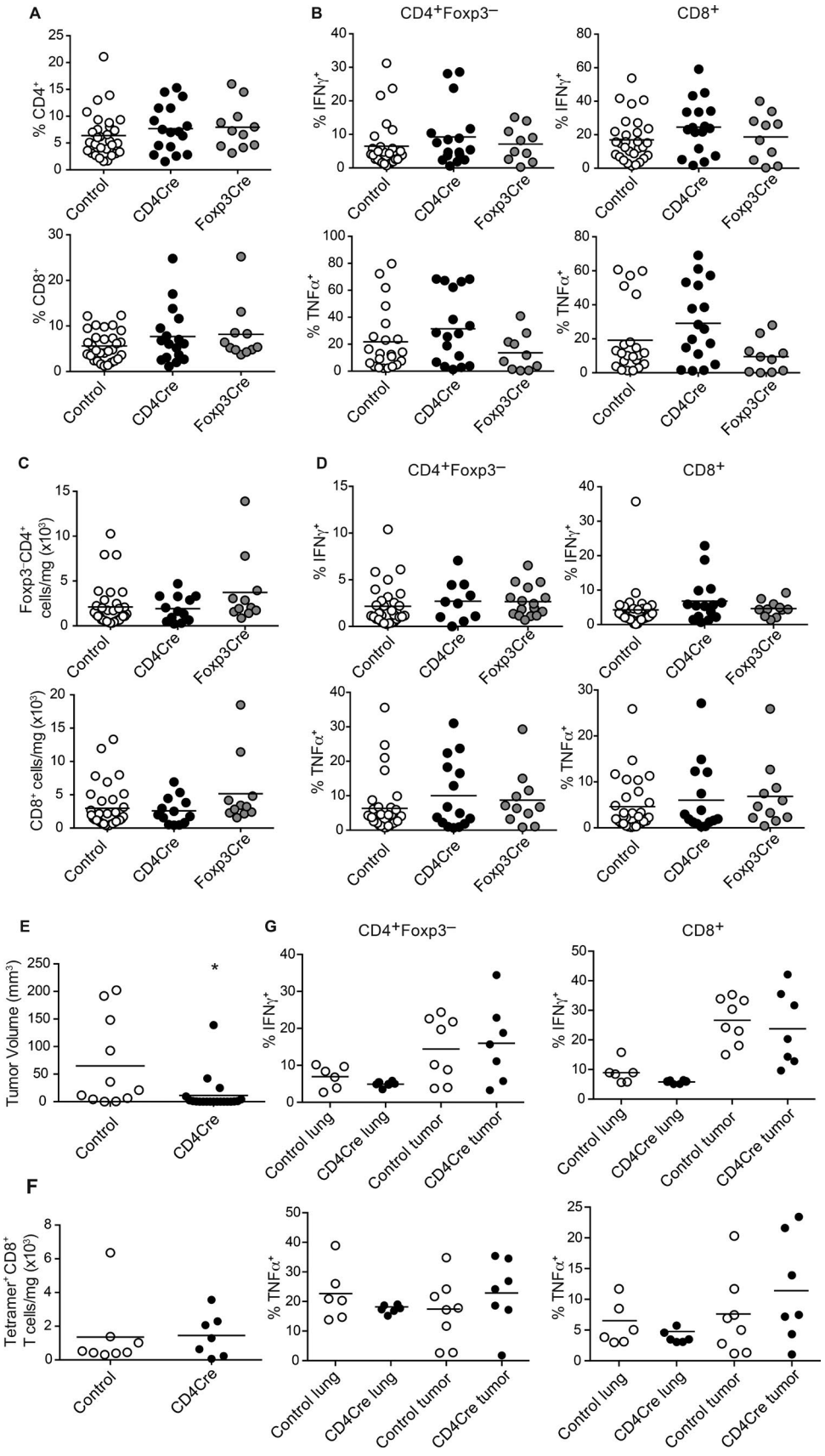

keratinocytes (Berasain et al., 2005; Brandl et al., 2010; Stoll et al., 2010). Areg has also been linked to human cancer as an oncogenic factor (Busser et al., 2010). In non–small cell lung cancers, Areg overexpression correlates with resistance to anti-ErbB agents that interfere with EGFR signaling (Li et al., 2009; Busser et al., 2010). Our studies indicate that T cell–produced Areg is not acting directly on the tumor cells, but likely on other tumor-resident cells, including macrophages, neutrophils, or lung epithelial cells, which act as intermediates in promoting tumor growth.

Collectively, our results suggest a novel nonimmune mode of action for intratumoral T reg and "non–T reg" T cells in facilitating tumor growth through provision of tissue maintenance factors, such as amphiregulin. We propose that the tissue repair capacity of T cells can serve as a novel therapeutic target, which, when combined with the rapidly evolving strategies of boosting proinflammatory immune responses, will increase the efficacy of T cell–based cancer immunotherapies.

MATERIALS AND METHODS

Mice

Foxp3^{GFP} (Fontenot et al., 2005), *Foxp3*^{DTR} (Kim et al., 2007), *Foxp3*$^{YFP\text{-}Cre}$ (Rubtsov et al., 2008), *Areg*$^{FL/FL}$ (Arpaia et al., 2015), and CD4-cre transgenic mice (Sawada et al., 1994) have been previously described. All mouse studies were performed under protocol 08-10-023 approved by the Sloan Kettering Institute Institutional Animal Care and Use Committee. All mouse strains were maintained in the Sloan Kettering Institute animal facility in accordance with institutional guidelines.

Tumor experiments

LLC cells were a gift from J. Massague (Memorial Sloan Kettering Cancer Center, New York, NY). EO771 cells were purchased from CH3 Biosystems. B16-F10 cells were a gift from C. Ariyan (Memorial Sloan Kettering Cancer Center). All cell lines were grown in DMEM supplemented with 10% FBS, 1% L-glutamine, 1% penicillin-streptomycin, and 10 mM Hepes. For measurement of *Areg* expression, RNA from tumor cells was extracted in Trizol reagent (Life Technologies), and quantitative real-time PCR was performed with primers specific for *Areg* (forward, 5′-GCAAAAATGGAAAAGGCAGA-3′, and reverse, 5′-TGTCATCCTCGCTGTGAGTC-3′) and *Hprt* (forward, 5′-TCAGTCAACGGGGGACATAAA-3′, and reverse, 5′-GGGGCTGTACTGCTTAACCAG-3′).

For tumor cell transplantation, tumor cells were harvested in 0.05% trypsin, washed, and resuspended in DMEM without serum before counting. Cells were diluted in DMEM so that 200 µl could be injected into the tail veins of recipient mice. For T reg cell ablation experiments, DT (Sigma-Aldrich) was diluted to 2.5 µg/ml, and 200 µl (0.5 µg) was injected intravenously into mice that had received LLC cells previously. Tumors were measured under a microdissection microscope, and individual tumor volumes were calculated using the formula $V = 4/3\pi(\text{length}/2)(\text{width}/2)(\text{height}/2)$. Individual tumor volumes were summed for total tumor volume per mouse.

Cell isolation

Lymphocytes were isolated from lung and tumor tissue by digestion with collagenase A (1 mg/ml; Roche) and DNase I (0.5 µg/ml; Roche) in isolation buffer (RPMI 1640 supplemented with 5% FBS, 1% L-glutamine, 1% penicillin-streptomycin, and 10 mM Hepes) for 30 min at 37°C. Cells were filtered through 100-µm cell strainers, washed in isolation buffer, and stained in PBS supplemented with 0.25% BSA, 2 mM EDTA, and 0.1% sodium azide. Antibodies used included anti-CD45, anti-Foxp3, anti–IL-18Rα, anti-ST2, anti-CD62L, anti-CD103, anti–PD-1, anti-GITR, anti–CTLA-4, anti-KLRG1, anti-Ki67, anti-CD5, anti-NK1.1, anti-CD45R (B220), anti–IL-17, anti–IL-4, anti-IFNγ, and anti–Ly-6C (eBioscience); anti-TCRβ, anti-CD3, anti-CD4, anti-CD8, anti-CD127, anti-CD11B, anti-MHCII, and anti-Gr1 (BioLegend); anti-CD44 and anti-CD25 (Tonbo); anti–IL-5 and anti-TNFα (BD PharMingen); and anti-AREG (R&D Systems). For exclusion of dead cells, samples were first stained with Ghost Dye (Tonbo) cell viability reagent. Intracellular staining for cytokines, Foxp3, AREG, Ki-67, and CTLA-4 was performed using the Foxp3/transcription factor staining buffer set (eBioscience) as per manufacturer's protocol. The H2-K^b OVA$_{257–264}$ tetramer was obtained from the NIH Tetramer Core Facility.

Ex vivo stimulation

To measure T cell production of Areg and cytokines, cells were treated where noted with PMA (50 ng/ml; Sigma) and ionomycin (1 nM; Calbiochem) for 3 h in the presence of GolgiPlug (brefeldin A) and GolgiStop (monensin; BD Biosciences) or stained directly ex vivo after isolation from lungs or tumors.

Figure 4. **T cell–derived Areg does not impact immune status in lung tumors.** (A–D) Flow cytometric analysis of T cell responses in control (*Areg*$^{FL/FL}$ or *Areg*$^{FL/WT}$), *Areg*$^{FL/FL}$CD4-cre, and *Areg*$^{FL/FL}$*Foxp3*$^{YFP\text{-}cre}$ mice at day 22–24. Percentages of total (A and C) and IFNγ- and TNFα-producing (B and D) CD4$^+$ and CD8$^+$ T cells within LLC (A and B) and EO771 (C and D) tumors of indicated mice; $n > 10$ mice per group each pooled from two to three independent experiments. (E–G) *Areg*$^{FL/FL}$ control and *Areg*$^{FL/FL}$ × CD4-cre were injected with 250,000 LLC-OVAp cells. Tumors were analyzed at day 22–24. (E) Tumor size in mice of indicated group. $n = 11–20$ mice per group, pooled from two independent experiments; *, $P < 0.01$. (F) Numbers of OVA-specific CD8$^+$ T cells in tumors assessed by staining with OVAp-K^b tetramer. (G) Percentages of Foxp3$^-$CD4$^+$ and CD8$^+$ T cells producing IFNγ and TNFα in LLC-OVAp tumors of indicated mice. In F and G, $n = 6–8$ mice per group, pooled from two independent experiments. Horizontal lines indicate the mean.

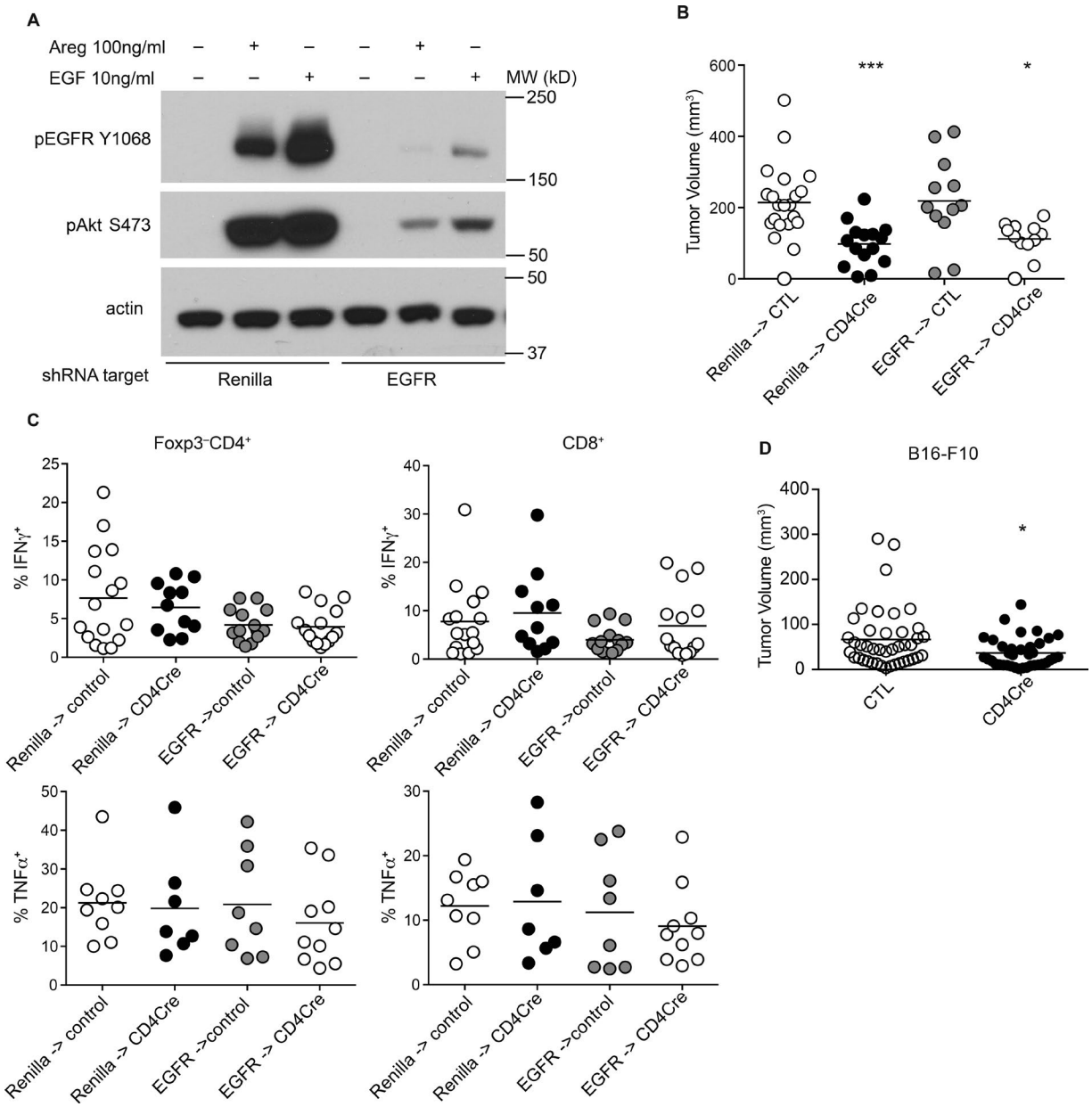

Figure 5. **T cell–derived Areg contributes to tumor growth indirectly.** (A) Western blot showing levels of Akt and EGFR activation upon in vitro treatment of EO771 cells with either Areg or EGF for 10 min. (B) 250,000 EGFR or control shRNA–expressing EO771 cells were injected into *Areg*$^{FL/FL}$ control and *Areg*$^{FL/FL}$CD4-cre mice, and tumors were analyzed at day 24–26. Tumor size in mice of indicated groups is shown; *n* = 12–21 mice per group, pooled from three independent experiments; *, P < 0.05; ***, P < 0.001. (C) Percentages of IFNγ- and TNFα-producing Foxp3^{-}CD4^{+} and CD8^{+} T cells in EO771-shRNA tumors of indicated mice; *n* = 8–10 mice per group, pooled from two independent experiments. (D) 150,000 B16-F10 cells were injected i.v. into *Areg*$^{FL/FL}$ control and *Areg*$^{FL/FL}$CD4-cre mice, and tumors were analyzed at day 22–24. Tumor size in mice of indicated groups is shown; *n* = 38–42 mice per group, pooled from four independent experiments; *, P < 0.05. Horizontal lines indicate the mean.

RNA sequencing

Foxp3^{+}CD4^{+}CD3^{+} T reg cells and Foxp3^{-}CD4^{+}CD3^{+} effector T cells isolated from lungs and tumors of *Foxp3*^{GFP} mice bearing LLC tumors 21 d after transplantation were distinguished on the basis of GFP expression and antibody staining and FACS-sorted directly into TRIzol LS reagent (Life Technologies). Three biological replicates of each population were isolated. Extracted RNA was amplified by SMART amplification (Clontech). Total RNA was used for poly(A) selection and to create Ion Torrent–compatible libraries using the Ion ChIP-Seq kit starting with the end-repair process (Life Technologies), with 12–16 cycles of PCR.

The resulting barcoded samples were loaded onto template-positive Ion PITM Ion SphereTM Particles using the Ion One Touch system II and Ion PITMTemplate OT2 200kit v2 kit (Life Technologies). Enriched particles were sequenced on a Proton sequencing system using the 200-bp version 2 chemistry. A mean of 70 to 80 million single-end reads were generated per sample. Raw reads were trimmed using Trimmomatic v0.32 with standard settings to remove low-quality reads and adaptor contamination. The trimmed reads were then aligned to the mouse genome (Ensembl assembly GRCm38) using TopHat2 v2.0.11 implementing Bowtie2 v2.2.2 with default settings. Read alignments were sorted with SAMtools v0.1.19 before being counted to genomic features using HTSeq v0.6.1p1. Pathway analysis of genes differentially up-regulated in tumor T reg cells compared with normal lung T reg cells using the GOrilla tool (http://cbl-gorilla.cs.technion.ac.il/) showed that this gene set was enriched for those involved in cellular migration and localization and cellular proliferation, as well as inflammatory responses.

Histology

Tumor-bearing lungs were fixed in 4% paraformaldehyde, embedded in paraffin, and sectioned before staining using the Leica BOND Automated Immunostainer (Leica Biosystems). Sections were stained with DAPI and antibodies against cleaved caspase-3, Ki-67, CD31, CD3, Foxp3, and CD11b. Images were acquired using a Zeiss Axioplan2 microscope. Regions of interest were drawn, and numbers of positive-staining cells and percentages of positive-staining area were quantified using Fiji software.

shRNA targeting

Oligomers of 97 base pairs targeting EGFR and Renilla luciferase were subcloned into the modified retroviral mir-30 backbone miR-E (Fellmann et al., 2013). Retrovirus produced in Phoenix-E cells was used to transduce EO771 or LLC cells, which were selected for shRNA expression on the basis of puromycin resistance by culture in 8 µg/ml puromycin: EGFR, 5′-TGCTGTTGACAGTGAGCGACCACGAGAACTAGAAATTCTATAGTGAAGCCACAGATGTATAGAATTTCTAGTTCTCGTGGGTGCCTACTGCCTCGGA-3′; AREG, 5′-TGCTGTTGACAGTGAGCGATCAGAGGAGTATGATAATGAATAGTGAAGCCACAGATGTATTCATTATCATACTCCTCTGAGTGCCTACTGCCTCGGA-3′; and Renilla, 5′-TGCTGTTGACAGTGAGCGCAGGAATTATAATGCTTATCTATAGTGAAGCCACAGATGTATAGATAAGCATTATAATTCCTATGCCTACTGCCTCGGA-3′.

Knockdown of EGFR expression and signaling was verified by Western blot after 10-min stimulation of cells serum-starved overnight with recombinant mouse EGF or rmAreg (BioLegend) followed by lysis in 20 mM Tris-HCl, 150 mM NaCl, 1 mM EDTA, 1 mM EGTA, 1% Triton X-100, cOmplete protease inhibitor cocktail (Sigma-Aldrich), and PhosSTOP phosphatase inhibitor cocktail (Sigma-Aldrich). Lysates were separated by SDS-PAGE, transferred to PVDF membranes, and probed with antibodies against β-actin (Sigma-Aldrich), phospho-Akt S473, phospho-EGFR Y1068, and phosphor-ERK1/2 T202/Y204 (Cell Signaling Technology).

Statistical analysis

All statistical analyses (excluding RNA-seq analyses) were performed using Prism 6 (GraphPad Software). Differences between individual groups were analyzed for statistical significance using unpaired two-tailed Student's *t* tests. *, $P \leq 0.05$; **, $P \leq 0.01$; ***, $P \leq 0.001$; ****, $P \leq 0.0001$.

Deposition of data

RNA sequencing data has been deposited with the NCBI BioProject database with project ID PRJNA400616.

Online supplemental material

Fig. S1 shows the production of Areg by T cells and non–T cells in LLC lung tumors. Fig. S2 shows the role of tumor-produced Areg in tumor progression. Fig. S3 shows EGFR signaling upon Areg stimulation in LLC and B16-F10 tumor cell lines.

ACKNOWLEDGMENTS

We thank members of the Rudensky laboratory for helpful discussions and advice, K.A. Kaiser for help with breeding mice and assistance with Areg knockdown experiments, the Memorial Sloan Kettering Cancer Center Molecular Cytology Core Facility for assistance with tissue staining and analysis, and A.H. Bravo and M.B. Faire for help with mouse colony management.

This work was supported by National Institutes of Health/National Cancer Institute Cancer Center Support Grant P30CA008748, National Institutes of Health Grant R37AI034206 (A.Y. Rudensky), the Ludwig Center at Memorial Sloan Kettering Cancer Center, the Hilton-Ludwig Cancer Prevention Initiative (Conrad N. Hilton Foundation and Ludwig Institute for Cancer Research; A.Y. Rudensky), an Irvington Fellowship of the Cancer Research Institute (J.A. Green), and the Robert Black Fellowship of the Damon Runyon Cancer Research Foundation (DRG-2143-13; N. Arpaia). A.Y. Rudensky is an investigator with the Howard Hughes Medical Institute.

The authors declare no competing financial interests.

Author contributions: J.A. Green, N. Arpaia, and A.Y. Rudensky conceived the study and designed experiments. J.A. Green and A.Y. Rudensky wrote the manuscript. J.A. Green and N. Arpaia performed experiments and analyzed data. M. Schizas assisted with RNA-seq data analysis. A. Dobrin assisted with immunofluorescence analysis.

Submitted: 23 February 2017

Revised: 2 August 2017

Accepted: 6 September 2017

REFERENCES

Arpaia, N., J.A. Green, B. Moltedo, A. Arvey, S. Hemmers, S. Yuan, P.M. Treuting, and A.Y. Rudensky. 2015. A distinct function of regulatory T cells in tissue protection. *Cell.* 162:1078–1089. https://doi.org/10.1016/j.cell.2015.08.021

Berasain, C., and M.A. Avila. 2014. Amphiregulin. *Semin. Cell Dev. Biol.* 28:31–41. https://doi.org/10.1016/j.semcdb.2014.01.005

Berasain, C., E.R. García-Trevijano, J. Castillo, E. Erroba, M. Santamaría, D.C. Lee, J. Prieto, and M.A. Avila. 2005. Novel role for amphiregulin in

protection from liver injury. *J. Biol. Chem.* 280:19012–19020. https://doi.org/10.1074/jbc.M413344200

Bos, P.D., G. Plitas, D. Rudra, S.Y. Lee, and A.Y. Rudensky. 2013. Transient regulatory T cell ablation deters oncogene-driven breast cancer and enhances radiotherapy. *J. Exp. Med.* 210:2435–2466. https://doi.org/10.1084/jem.20130762

Brandl, K., L. Sun, C. Neppl, O.M. Siggs, S.M. Le Gall, W. Tomisato, X. Li, X. Du, D.N. Maennel, C.P. Blobel, and B. Beutler. 2010. MyD88 signaling in nonhematopoietic cells protects mice against induced colitis by regulating specific EGF receptor ligands. *Proc. Natl. Acad. Sci. USA.* 107:19967–19972. https://doi.org/10.1073/pnas.1014669107

Burzyn, D., W. Kuswanto, D. Kolodin, J.L. Shadrach, M. Cerletti, Y. Jang, E. Sefik, T.G. Tan, A.J. Wagers, C. Benoist, and D. Mathis. 2013. A special population of regulatory T cells potentiates muscle repair. *Cell.* 155:1282–1295. https://doi.org/10.1016/j.cell.2013.10.054

Busser, B., L. Sancey, V. Josserand, C. Niang, M.C. Favrot, J.L. Coll, and A. Hurbin. 2010. Amphiregulin promotes BAX inhibition and resistance to gefitinib in non-small-cell lung cancers. *Mol. Ther.* 18:528–535. https://doi.org/10.1038/mt.2009.226

Chen, D.S., and I. Mellman. 2013. Oncology meets immunology: The cancer-immunity cycle. *Immunity.* 39:1–10. https://doi.org/10.1016/j.immuni.2013.07.012

Daniel, D., N. Meyer-Morse, E.K. Bergsland, K. Dehne, L.M. Coussens, and D. Hanahan. 2003. Immune enhancement of skin carcinogenesis by $CD4^+$ T cells. *J. Exp. Med.* 197:1017–1028. https://doi.org/10.1084/jem.20021047

Fellmann, C., T. Hoffmann, V. Sridhar, B. Hopfgartner, M. Muhar, M. Roth, D.Y. Lai, I.A. Barbosa, J.S. Kwon, Y. Guan, et al. 2013. An optimized microRNA backbone for effective single-copy RNAi. *Cell Reports.* 5:1704–1713. https://doi.org/10.1016/j.celrep.2013.11.020

Fontenot, J.D., J.P. Rasmussen, L.M. Williams, J.L. Dooley, A.G. Farr, and A.Y. Rudensky. 2005. Regulatory T cell lineage specification by the forkhead transcription factor foxp3. *Immunity.* 22:329–341. https://doi.org/10.1016/j.immuni.2005.01.016

Fridman, W.H., F. Pagès, C. Sautès-Fridman, and J. Galon. 2012. The immune contexture in human tumours: Impact on clinical outcome. *Nat. Rev. Cancer.* 12:298–306. https://doi.org/10.1038/nrc3245

Gooden, M.J., G.H. de Bock, N. Leffers, T. Daemen, and H.W. Nijman. 2011. The prognostic influence of tumour-infiltrating lymphocytes in cancer: A systematic review with meta-analysis. *Br. J. Cancer.* 105:93–103. https://doi.org/10.1038/bjc.2011.189

Hofmann, U., N. Beyersdorf, J. Weirather, A. Podolskaya, J. Bauersachs, G. Ertl, T. Kerkau, and S. Frantz. 2012. Activation of CD4+ T lymphocytes improves wound healing and survival after experimental myocardial infarction in mice. *Circulation.* 125:1652–1663. https://doi.org/10.1161/CIRCULATIONAHA.111.044164

Hopewell, E.L., W. Zhao, W.J. Fulp, C.C. Bronk, A.S. Lopez, M. Massengill, S. Antonia, E. Celis, E.B. Haura, S.A. Enkemann, et al. 2013. Lung tumor NF-κB signaling promotes T cell-mediated immune surveillance. *J. Clin. Invest.* 123:2509–2522. https://doi.org/10.1172/JCI67250

Kim, J.M., J.P. Rasmussen, and A.Y. Rudensky. 2007. Regulatory T cells prevent catastrophic autoimmunity throughout the lifespan of mice. *Nat. Immunol.* 8:191–197. https://doi.org/10.1038/ni1428

Klages, K., C.T. Mayer, K. Lahl, C. Loddenkemper, M.W. Teng, S.F. Ngiow, M.J. Smyth, A. Hamann, J. Huehn, and T. Sparwasser. 2010. Selective depletion of Foxp3+ regulatory T cells improves effective therapeutic vaccination against established melanoma. *Cancer Res.* 70:7788–7799. https://doi.org/10.1158/0008-5472.CAN-10-1736

Li, C., M. Iida, E.F. Dunn, A.J. Ghia, and D.L. Wheeler. 2009. Nuclear EGFR contributes to acquired resistance to cetuximab. *Oncogene.* 28:3801–3813. https://doi.org/10.1038/onc.2009.234

Nosbaum, A., N. Prevel, H.A. Truong, P. Mehta, M. Ettinger, T.C. Scharschmidt, N.H. Ali, M.L. Pauli, A.K. Abbas, and M.D. Rosenblum. 2016. Cutting edge: Regulatory T cells facilitate cutaneous wound healing. *J. Immunol.* 196:2010–2014. https://doi.org/10.4049/jimmunol.1502139

Pastille, E., K. Bardini, D. Fleissner, A. Adamczyk, A. Frede, M. Wadwa, D. von Smolinski, S. Kasper, T. Sparwasser, A.D. Gruber, et al. 2014. Transient ablation of regulatory T cells improves antitumor immunity in colitis-associated colon cancer. *Cancer Res.* 74:4258–4269. https://doi.org/10.1158/0008-5472.CAN-13-3065

Rubtsov, Y.P., J.P. Rasmussen, E.Y. Chi, J. Fontenot, L. Castelli, X. Ye, P. Treuting, L. Siewe, A. Roers, W.R. Henderson Jr., et al. 2008. Regulatory T cell-derived interleukin-10 limits inflammation at environmental interfaces. *Immunity.* 28:546–558. https://doi.org/10.1016/j.immuni.2008.02.017

Sadtler, K., K. Estrellas, B.W. Allen, M.T. Wolf, H. Fan, A.J. Tam, C.H. Patel, B.S. Luber, H. Wang, K.R. Wagner, et al. 2016. Developing a pro-regenerative biomaterial scaffold microenvironment requires T helper 2 cells. *Science.* 352:366–370. https://doi.org/10.1126/science.aad9272

Sawada, S., J.D. Scarborough, N. Killeen, and D.R. Littman. 1994. A lineage-specific transcriptional silencer regulates CD4 gene expression during T lymphocyte development. *Cell.* 77:917–929. https://doi.org/10.1016/0092-8674(94)90140-6

Schäfer, M., and S. Werner. 2008. Cancer as an overhealing wound: An old hypothesis revisited. *Nat. Rev. Mol. Cell Biol.* 9:628–638. https://doi.org/10.1038/nrm2455

Stoll, S.W., J.L. Johnson, Y. Li, L. Rittié, and J.T. Elder. 2010. Amphiregulin carboxy-terminal domain is required for autocrine keratinocyte growth. *J. Invest. Dermatol.* 130:2031–2040. https://doi.org/10.1038/jid.2010.98

Tan, W., W. Zhang, A. Strasner, S. Grivennikov, J.Q. Cheng, R.M. Hoffman, and M. Karin. 2011. Tumour-infiltrating regulatory T cells stimulate mammary cancer metastasis through RANKL-RANK signalling. *Nature.* 470:548–553. https://doi.org/10.1038/nature09707

Weirather, J., U.D. Hofmann, N. Beyersdorf, G.C. Ramos, B. Vogel, A. Frey, G. Ertl, T. Kerkau, and S. Frantz. 2014. Foxp3+ CD4+ T cells improve healing after myocardial infarction by modulating monocyte/macrophage differentiation. *Circ. Res.* 115:55–67. https://doi.org/10.1161/CIRCRESAHA.115.303895

Zaiss, D.M., J. van Loosdregt, A. Gorlani, C.P. Bekker, A. Gröne, M. Sibilia, P.M. van Bergen en Henegouwen, R.C. Roovers, P.J. Coffer, and A.J. Sijts. 2013. Amphiregulin enhances regulatory T cell-suppressive function via the epidermal growth factor receptor. *Immunity.* 38:275–284. https://doi.org/10.1016/j.immuni.2012.09.023

Zhang, N., Y. Zeng, W. Du, J. Zhu, D. Shen, Z. Liu, and J.A. Huang. 2016. The EGFR pathway is involved in the regulation of PD-L1 expression via the IL-6/JAK/STAT3 signaling pathway in EGFR-mutated non-small cell lung cancer. *Int. J. Oncol.* 49:1360–1368. https://doi.org/10.3892/ijo.2016.3632